

## Accepted Manuscript

Highly delayed systemic translocation of aluminium-based adjuvant in CD1 mice following intramuscular injections

Guillemette Crépeaux, Housam Eidi, Marie-Odile David, Eleni Tzavara, Bruno Giros, Christopher Exley, Patrick A. Curmi, Christopher A. Shaw, Romain K. Gherardi, Josette Cadusseau

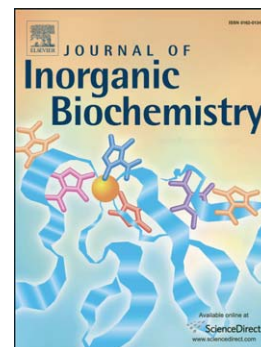
PII: S0162-0134(15)30031-3  
DOI: doi: [10.1016/j.jinorgbio.2015.07.004](https://doi.org/10.1016/j.jinorgbio.2015.07.004)  
Reference: JIB 9757

To appear in: *Journal of Inorganic Biochemistry*

Received date: 30 April 2015  
Revised date: 8 July 2015  
Accepted date: 9 July 2015

Please cite this article as: Guillemette Crépeaux, Housam Eidi, Marie-Odile David, Eleni Tzavara, Bruno Giros, Christopher Exley, Patrick A. Curmi, Christopher A. Shaw, Romain K. Gherardi, Josette Cadusseau, Highly delayed systemic translocation of aluminium-based adjuvant in CD1 mice following intramuscular injections, *Journal of Inorganic Biochemistry* (2015), doi: [10.1016/j.jinorgbio.2015.07.004](https://doi.org/10.1016/j.jinorgbio.2015.07.004)

This is a PDF file of an unedited manuscript that has been accepted for publication. As a service to our customers we are providing this early version of the manuscript. The manuscript will undergo copyediting, typesetting, and review of the resulting proof before it is published in its final form. Please note that during the production process errors may be discovered which could affect the content, and all legal disclaimers that apply to the journal pertain.



**Highly delayed systemic translocation of aluminium-based adjuvant in CD1 mice following intramuscular injections.**

**Guillemette Crépeaux<sup>1\*</sup>, Housam Eidi<sup>1,2</sup>, Marie-Odile David<sup>2</sup>, Eleni Tzavara<sup>3</sup>, Bruno Giros<sup>3</sup>, Christopher Exley<sup>4</sup>, Patrick A Curmi<sup>2</sup>, Christopher A Shaw<sup>5\*</sup>, Romain K Gherardi<sup>1°</sup>, Josette Cadusseau<sup>1,6°</sup>.**

<sup>1</sup>Inserm U955 E10, Paris Est University, Créteil, France.

<sup>2</sup>Inserm U829, Evry University, Evry, France.

<sup>3</sup>Inserm U1130, Cnrs UMR 8246, UPMC UM CR18, Paris, France.

<sup>4</sup>Birchall Centre, Keele University, Staffordshire, UK.

<sup>5</sup>Department of Ophthalmology, University of British Columbia, Vancouver, BC, Canada.

<sup>6</sup>Faculté des Sciences & Technologie UPEC, Créteil, France.

<sup>°</sup> These authors contributed equally to this work.<sup>1</sup>

---

\*Corresponding author: guillemette.crepeaux@gmail.com fax +33 1 49 81 36 42

**Abstract**

Concerns regarding vaccine safety have emerged following reports of potential adverse events in both humans and animals. In the present study, alum, alum-containing vaccine and alum adjuvant tagged with fluorescent nanodiamonds were used to evaluate i) the persistence time at the injection site, ii) translocation of alum from the injection site to lymphoid organs, iii) behaviour of adult CD1 mice following intramuscular injection of alum (400 µg Al/kg). Results showed for the first time a strikingly delayed systemic translocation of adjuvant particles. Alum-induced granuloma remained for a very long time in the injected muscle despite progressive shrinkage from day 45 to day 270. Concomitantly, a markedly delayed translocation of alum to the draining lymph nodes, major at day 270 endpoint, was observed. Translocation to the spleen was similarly delayed (highest number of particles at day 270). In contrast to C57BL/6J mice, no brain translocation of alum was observed by day 270 in CD1 mice. Consistently neither increase of Al cerebral content, nor behavioural changes were observed. On the basis of previous reports showing alum neurotoxic effects in CD1 mice, an additional experiment was done, and showed early brain translocation at day 45 of alum injected subcutaneously at 200 µg Al/kg. This study confirms the striking biopersistence of alum. It points out an unexpectedly delayed diffusion of the adjuvant in lymph nodes and spleen of CD1 mice, and suggests the importance of mouse strain, route of administration, and doses, for futures studies focusing on the potential toxic effects of aluminium-based adjuvants.

**Keywords:** Alum, vaccine-adjuvant, fluorescent-nanodiamonds, delayed-translocation, neurotoxicity, CD1 mice.

## Introduction

Aluminium (Al) is the third most abundant element in the Earth's crust and it is ubiquitously present in our everyday life in a great variety of objects (cooking utensils, food packaging, housing materials, pharmaceutical products, cosmetics, etc). Al is found in all body fluids (blood, cerebral spinal fluid, interstitial fluid of the brain, lymph, sweat, seminal fluids and urine) [1]. Despite the widespread use of Al in our environment leading to this increase of its bioavailability, Al has no known biological role [2].

Furthermore, it is widely accepted that Al and Al compounds are neurotoxic for animals and humans [3,4]. For instance, Al exposure has been implicated in the pathology of several neurodegenerative diseases associated with cognitive impairments, as Alzheimer's disease [5-7]. The molecular mechanisms by which it causes neuronal damage are not fully understood [8], but it is generally accepted that the nervous system is particularly sensitive to oxidant-mediated damage [9], and that the neurotoxicity of Al is caused by its ability to increase oxidative damage in the brain [10].

Finally, the bioavailability of Al, its ability to cross the blood-brain barrier, and the relatively slow rate of elimination from the brain contribute to progressive accumulation of Al into the brain [11-13], and enhance neurotoxicological risk [14].

Many severe infectious diseases can be prevented by vaccine and some of them have been eradicated. Furthermore novel vaccine strategies are now being developed as promising therapies to overcome diseases such as cancer. However, though vaccines are commonly and safely used, and are generally well tolerated by most people, they occasionally cause adverse effects, such as ill-defined conditions usually manifesting as symptoms such as myalgia, arthralgia, chronic fatigue and development of autoantibodies [15]. No consensus exists so far on a cause-to-effect relationship, but vaccine adjuvants have been suspected to be associated

with several inflammatory/neurodegenerative or autoimmune conditions impacting the central nervous system such as multiple sclerosis [16], amyotrophic lateral sclerosis [17] and autism [6]. A new syndrome has thus been identified by Shoenfeld in 2011, the autoimmune/auto-inflammatory syndrome induced by adjuvants (ASIA) [18].

Several papers from the literature suggest that vaccines containing aluminium adjuvants may be insidiously unsafe over the long-term. This is in line with the role of environmental aluminium that is continuously suspected to represent a possible co-factor of several chronic diseases [19-21,1].

Among unusual reactions to Aluminium hydroxide (alum) containing vaccines, macrophagic myofasciitis (MMF) is an inflammatory lesion described in 1998 [22], and recognized as a “distinctive histopathological entity that may be caused by intramuscular injection of Al-containing vaccines” [23].

MMF affects mainly women (>70% of total known cases), and is characterized by highly specific myopathological alterations observed in patients suffering from a combination of diffuse myalgias, arthralgia, chronic fatigue and cognitive impairment such as alterations affecting working memory and attention [22,24-27].

Alum-adjuvanted vaccines are usually administered in France through intramuscular injection into the deltoid muscle in adults [28]. In MMF patients deltoid muscle biopsies showed crystalline cytoplasmic inclusions in macrophages corresponding to alum agglomerates of vaccine origin [29]. The constant detection of these agglomerates in MMF assesses the unusually long persistence time of alum in affected individuals [30].

Both Al oxyhydroxide and Al hydroxyphosphate are used as vaccine adjuvants [31,32]. Indeed, Al has been added to vaccines since the early part of the twentieth century to enhance

the primary immunization [33]. The role of Al adjuvants was believed to prolong the retention of adsorbed antigens at the injection site, thus reducing the amount of antigen needed per dose and the number of required doses [34,35]. However, the “depot” theory has been challenged by early ablation of the injected site [36] and mechanisms of alum immunopotentiality only begin to be progressively understood [31].

Al containing vaccines are commonly used, such as vaccines against tetanus, hepatitis A, hepatitis B, human papillomavirus, haemophilus influenzae B, pneumococcal and meningococcal infections, and anthrax [37]. FDA regulations limit the Al content of an individual vaccinal dose to 0.85 mg of elemental Al [38].

Previous results have shown that Al particles, as other poorly degradable particles, do not stay localized in the injected muscle tissue, but can rather disseminate within phagocyte cells to lymph nodes and distant sites including spleen and brain [39]. A previous study of our group looked at aluminium translocation after intramuscular injection of alum-containing vaccine in C57BL/6J mice. Aluminium was detected in the injected muscle, but also in distant organs such as the spleen, a few days after injection, and then in the brain where it was still detected one year later. Using surrogate labeled particles containing precipitated alum, a rapid phagocytosis of injected particles by muscle monocyte lineage cells and their translocation via lymph and blood vessels were confirmed. Particles reached the brain as soon as 3 weeks post-injection and were shown to accumulate albeit very slowly and in small numbers [39]. Recently, we developed a new tool allowing tracing of  $\text{Al}(\text{OH})_3$  particles in tissues at very low levels and over the long-term [40]. This method consists of tagging Al adjuvant itself (Alhydrogel<sup>®</sup>) with fluorescent nanodiamonds (fNDs) functionalized with hyperbranched polyglycerol (HPG). The complex alum-nanodiamonds (AluDia) had physico-chemical properties similar to HBV vaccine [40]. When injected in the *tibialis anterior* (TA) muscle of

C57BL/6J mice, it allowed the monitoring of lymphatic and systemic biodistribution of AluDia particles and their presence in brain tissue, 3 weeks after the intramuscular injection.

The potential impact of aluminium adjuvant on the nervous system has been studied in mouse models. Aluminium adjuvant, dosed at 100  $\mu\text{g Al/kg}$  and subcutaneously injected in CD1 mice, induced motor deficits and anxiety increases associated with motor neuron death and astrogliosis [17]. Although no motoneuron death was observed when the dose was increased 3-fold, Shaw and Petrik [41] observed a microglial and astrocytic reactivity in the spinal cord of CD1 mice that present with an increase in anxiety, significant impairments in a number of motor functions and diminished spatial memory capacity. A neuroinflammatory syndrome has been described in sheep after the repetitive administration of Al-containing vaccines [42]. Recently, impairment of neurocognitive functions and brain gliosis were reported in a murine model of Systemic Lupus Erythematosus-like disease following intramuscular injection of Al hydroxide or vaccine against the hepatitis B virus (HBV) (200  $\mu\text{g/mouse}$ ) [43].

Although progressive shrinkage of the local granuloma [44,45] and rapid translocation of alum from the injected site to draining lymph nodes (dLNs) and spleen have been repeatedly demonstrated [39,40], long-term biodisposition of alum particles trapped in the local granuloma remains unexplored. To examine this point we designed a longitudinal study in which alum, alum-containing vaccine and alum tagged with fluorescent nanodiamonds were used in adult CD1 mice to evaluate i) the persistence time at the injection site, ii) long-term translocation of alum from the injection site to lymphoid organs, and iii) behaviour and motricity of animals following intramuscular injection of alum.

## 1. Materials and methods

### 1.1. Dose of exposure

The dose of 400  $\mu\text{g}$  Al/kg was chosen to model a plurivaccination with the HBV ENGERIX<sup>®</sup> vaccine. Medical histories of MMF patients revealed that 100% (50/50 patients) of them received 1-9 (median 4) doses of an Al-containing vaccine within 10 years prior to their diagnosis [29]. A 60-kg woman injected with 1 dose of HBV ENGERIX<sup>®</sup> vaccine receives 500  $\mu\text{g}$  of Al, i.e. 8.3  $\mu\text{g}$  Al/kg of body weight. The allometric conversion from human to mouse (FDA guidance 5541) gives a final amount of approximately 100  $\mu\text{g}$  Al/kg. 400  $\mu\text{g}$  Al/kg was used to mimic a cumulative effect induced by 4 shots.

### 1.2. Animals

155 female CD1 mice, weighing 25-30 g (7 weeks old), were obtained from Charles Rivers Laboratories (France). Upon arrival, the females were housed at 5 per cage. Animals were maintained under a 12:12 light cycle, at a constant temperature ( $22 \pm 2^\circ\text{C}$ ) and a relative humidity of  $55 \pm 10\%$ . Mice were protected from Al-containing materials and were given free access to food and water. After a 1-week period for acclimatization, mice were separated in two experimental series.

All these experiments on animals were performed in respect with the guidelines provided by the European Union (Directive 2010/63/EU) [46].

### ***AluDia translocation series***

After the acclimatization period, 35 8-week old females were separated into 7 experimental groups of 5 animals each receiving 3 intra-muscular (im) injections in the left *tibialis anterior* muscle or 3 subcutaneous (sc) injections in the neck, each of 20  $\mu\text{L}$  with a 4-day interval between each injection. The 7 groups received AluDia: 200  $\mu\text{g Al/kg}$ , im; 400  $\mu\text{g Al/kg}$ , im; 200  $\mu\text{g Al/kg}$ , sc; 400  $\mu\text{g Al/kg}$ , sc. The AluDia complex used was identical to the one prepared by Eidi *et al.* [40]. Briefly, the functionalized fluorescent nanodiamonds (fNDs) were prepared by milling synthetic HPHT (High Pressure High Temperature) micron powder holding nitrogen-vacancy centers (at the origin of permanent fluorescence) created by electronic irradiation and annealing [47]. Afterwards, the fNDs are functionalized with hyper branched polyglycerol (HPG) synthesized from glycidol (Sigma Aldrich, Saint Quentin Fallavier, France) [48] which ensures the colloidal stability of the suspension in buffer and the formation of the complex with aluminic particles. The AluDia complex was prepared by mixing fND-HPG (1.3 g/L) and Alhydrogel<sup>®</sup> (10 g/L) suspensions at a ratio of 1:17 v/v and followed by a thorough agitation and a few minutes sonication. AluDia suspension was then diluted to reach the appropriate concentration in PBS. In the physiological conditions we used, AluDia particle size and zeta potential were very similar to those of Alhydrogel<sup>®</sup> alone or HBV vaccine [40].

### ***Adjuvant/vaccine series***

After the acclimatization period, 120 8-week old females were separated into 3 experimental subgroups of 40 animals each receiving 3 intra-muscular injections of 20  $\mu\text{L}$  in TA, with a 4-day interval between each injection.

The 3 groups were: Alhydrogel<sup>®</sup> group (400 µg Al/kg) (Invivogen, Toulouse, France); Vaccine HBV ENGERIX<sup>®</sup> group (400 µg Al/kg) (Glaxo, Rixensart, Belgium) and a PBS control group (Invivogen, Toulouse, France).

### ***Behavioural tests and end point for sacrifice***

Animals were enrolled in a battery of 8 complementary tests two weeks before the endpoint. At the end of the behavioural tests (45, 135, 180, 270 days post injection), animals were sacrificed with an overdose of pentobarbital (100-150 mg/kg, intra peritoneal injection) and samples (TA muscles, dLNs, spleen, and brain) were removed and quickly frozen in isopentane, then stored at -80°C until use. Precautions were taken to avoid external environmental aluminium contamination of samples.

Muscle samples of 3 animals from each group were dedicated to the analyses of the granuloma size in the injected muscle whereas brain samples of 5 animals were dedicated to the measurement of Al concentration.

#### 1.3. Muscle granuloma size at the injection site

The granuloma size was semi-quantitatively assessed on muscle sections stained with hematoxylin-eosin in treatment groups that received either the adjuvant Alhydrogel<sup>®</sup> or the HBV vaccine (n=3 muscles per group). Sections were observed with 20X objectives and granuloma were assessed according to their size. Four granuloma groups were determined: without granuloma (0), small (+), medium (++) and large (+++) granuloma. Then, the percentage of each size group was calculated at each time point.

#### 1.4. AluDia translocation

AluDia translocation from injection site to target organs (dLNs, spleen, and brain) was assessed as previously described by Eidi *et al.* [40] for 7 AluDia groups: 400  $\mu\text{g}$  Al/kg, im 45, 135, 180 or 270 days following injection; 200  $\mu\text{g}$  Al/kg, im, 200  $\mu\text{g}$  Al/kg, sc, and 400  $\mu\text{g}$  Al/kg, sc 45 days post injection.

##### ***Tissue preparation and particle counting***

Serial cryosections of muscle and spleen (20 $\mu\text{m}$  thick), inguinal lymph node (12 $\mu\text{m}$  thick) and brain (coronal plane, 40 $\mu\text{m}$  thick) were cut and stored at  $-20^{\circ}\text{C}$  until particle counting or treatment. Tissue sections were successively deposited on 10 different Superfrost<sup>®</sup>-plus slides in order to obtain 10 identical series. The total number of particles per organ was assessed by multiplying by 10 the number of particles found in a single series.

##### ***Epifluorescence microscopy and microspectrometry***

For fNDs detection, a DPSSL 532 nm (200 mW) laser beam was used as the illumination source and was guided to the microscope by a fiber optic. A long pass 600 nm emission filter was used to collect only wavelengths higher than 600 nm. Fluorescence images were obtained with a Princeton Instruments EMCCD Camera Roleraem-c<sup>2</sup>, with typical exposure times. Spectra of the fluorescent spots were acquired by focusing the fluorescent object emission from the microscope onto an Acton SP2150i spectrometer (Princeton instruments), and detected with a PIXIS-100B-eXcelon CCD camera (Princeton instruments).

### 1.5. Brain Al concentration

Analyses were carried out on 5 brains per group (groups PBS, Alhydrogel<sup>®</sup> (400 µg Al/kg) and HBV vaccine (400 µg Al/kg), 45, 135, 180 or 270 days following injection, according to the published method of House et al. [49]. Significant precautions were taken throughout the study to minimize contamination. These included storage of all plastic-based laboratory-ware in 5% v/v conc. HCl and, before use, rinsing of all such apparatus in several volumes of ultrapure water (cond. < 0.067 mS cm<sup>-1</sup>). Where required, rinsed apparatus was air-dried in a dedicated incubator at 37°C. Al concentrations were determined by TH GFAAS in half brains dried to a constant weight at 37°C and digested in a microwave (MARS Xpress CEM Microwave Technology Ltd) in a mixture of 1 mL 15.8 M HNO<sub>3</sub> (Fischer Analytical Grade) and 1 mL of 30% w/v H<sub>2</sub>O<sub>2</sub> (BDH Aristar Grade). Digests were clear and colourless or light yellow with no visible precipitate or fatty residue. Upon cooling each digest was diluted to a total volume of 5 mL with ultrapure water.

Total Al was measured immediately post digestion using an AAnalyst 600 atomic absorption spectrometer with a transversely heated graphite atomizer (THGA) and longitudinal Zeeman-effect background corrector and an AS-800 autosampler with WinLab32 software (Perkin Elmer, UK). Standard THGA pyrolytically-coated graphite tubes with integrated L'Vov platform (Perkin Elmer, UK) were used. The Zeeman background corrected peak area of the atomic absorption signal was used for the determinations.

Results were expressed as µg Al/g tissue dry weight. Each determination was the arithmetic mean of three injections with a relative standard deviation <10%.

### 1.6. Behavioural and motor testing

A battery of 8 behavioural or physical tests were performed at 45, 135, 180 or 270 days after the third injection in groups PBS, Alhydrogel<sup>®</sup> (400 µg Al/kg) and HBV vaccine (400 µg Al/kg). Tests were chosen in order to assess locomotor activity in the open-field [50], level of anxiety in the o-maze [51,52], short-term memory in the novel object recognition test [53-56], muscular strength in the wire mesh hang [57] and grip strength test [58], locomotor coordination in the rotarod test [59], depression in the tail suspension test [60], and pain sensitivity in the hot plate test [61]. Detailed procedures can be found in the supplementary data.

### 1.7. Statistical analysis

Tissue Al data were analyzed using a non-parametric Kruskal-Wallis test and a Mann-Whitney procedure for multiple comparisons. Data from behavioural tests were analyzed using a one-way analysis of variance (one-way ANOVA). *Post hoc* comparisons have been performed using the Bonferroni's test when Anova was significant.

Significance was set at  $p < 0.05$ . All statistical analyses were carried out using SPSS 16.0 software (SPSS INC., Chicago, IL, USA).

## 2. Results

### 3.1. Muscle granuloma size at the injection site

Serial sections of the injected muscle 45, 135, 180 and 270 days after Alhydrogel<sup>®</sup> (400 µg Al/kg) or HBV vaccine (400 µg Al/kg) injection showed progressive shrinkage of muscle granuloma (Table 1). At D45 all animals had granuloma with a majority of sections showing a granuloma (93% for Alhydrogel<sup>®</sup>, 67% for HBV vaccine). At D270, in contrast to previous time points, one animal was free of granuloma and a majority of overall muscle sections showed no granuloma (65% for Alhydrogel<sup>®</sup>, 69% for HBV vaccine) (Table 1).

### 3.2. AluDia translocation to dLNs and spleen

The study of translocation of AluDia particles (400 µg Al/kg) from muscle to distant organs showed progressive increase of AluDia particles in inguinal dLNs from D45 to D270 after injection (Table 2). Indeed, 1145 and 115478 AluDia particles were counted in inguinal dLNs at D45 and D270, respectively (Fig. 1). At D270, this 100 fold increase appeared as striking accumulation of AluDia in interfollicular areas of dLNs (Table 2 and Fig. 1). In the same way, AluDia particles increased by 52 fold in spleen (15 to 785 particles) between D45 and D270 (Table 2 and Fig. 1). Of note, particle concentrations were still increasing at the D270 endpoint in both dLNs and spleen.

### 3.3. Brain translocation of AluDia and behavioural/motricity tests

Surprisingly, no particles were observed in brains at any analyzed times after im injection of AluDia (Table 2). Consistently, as assessed by furnace atomic absorption spectrometry, animals receiving im injection of Alhydrogel<sup>®</sup> (400 µg Al/kg) or HBV vaccine (400 µg Al/kg) showed no increase of cerebral Al<sup>3+</sup> level compared to control animals injected with PBS (Table 3). Similarly behavioural and motor tests yielded no salient changes in elevated o-maze, open field, novel object recognition test, wire mesh hang test, grip strength test, rotarod test, tail suspension test, and hot plate test (supplementary data).

Taking into account that neurotoxic effects were previously reported in CD1 mice after sc injection of Alhydrogel<sup>®</sup> at 100 µg Al/kg [17] and 300 µg Al/kg [41], we examined whether the route of administration or the dose could influence brain translocation of AluDia. We observed that 3 out of 4 CD1 mice injected by the sc route with 200 µg Al/kg showed particle incorporation into brain 45 days after injection (Table 4 and Fig. 2). Notably, this was not observed at higher dose (400 µg Al/kg) for the sc route, and at any dose for the im route.

## 4. Discussion

This longitudinal study showed that alum (Alhydrogel<sup>®</sup> or HBV vaccine) injected into muscle constantly induces a granuloma similar to MMF that shrinks with time with marked clearance of granulomatous lesions observed from D180 to D270. This is similar to what was previously observed with the AluDia complex [40]. Granuloma shrinkage in muscle was associated with concurrent replenishment of inguinal dLNs (100 fold increase of AluDia particles from D45 to D270). Similar translocation of alum from muscle to dLNs was previously observed at much earlier time points in C57BL/6J mice [39]. We assume that two

waves of lymphatic translocation may occur after im injection of alum: an early one peaking at D4 [39], and a markedly delayed one associated with muscle granuloma shrinkage observed in the present study thanks to a long-term evaluation not performed in previous studies. We assume that this delayed lymphatic draining flux is the normal way of clearance for alum trapped in the post-vaccinal granuloma. Similarly to translocation to dLNs, we observed markedly delayed AluDia translocation to spleen, with a maximum number of particles being detected in this organ at D270. Alum translocation from muscle to spleen was previously shown to assess particle exit from lymphatic pathways to blood stream [39]. Since spleen was previously shown to incorporate a first peak of particles at D7 post im injection in C57BL/6J mice [40], the present study suggests a delayed second wave of adjuvant translocation to spleen in line with that observed in dLNs.

The present study confirms that alum is extremely biopersistent [29,37] and that alum biopersistence can be observed in both the injected muscle and distant organs, including dLNs and spleen. Regarding the strong immunostimulatory effects of alum and the unrequired depot formation for its adjuvant activity [36], long-term biopersistence of alum in lymphoid organs is clearly undesirable, and may cast doubts on the exact level of long-term safety of alum-  
adjuvanted vaccines [37].

The lack of brain translocation alum after im injection of 400  $\mu\text{g}$  Al/kg was puzzling. Notably, neither elevated Al concentration in brain nor neurobehavioural changes were observed in these experimental conditions, ruling out significant translocation of soluble Al to brain in the absence of physical incorporation of alum particles, and the induction of neurobehavioral effects by chronic peripheral immune activation linked to persistence of alum within immune cells [35].

It is not excluded that the observed difference in the biodisposition of alum in C57BL/6J and CD1 mice, including diffusion kinetics and the occurrence of brain translocation, may in part reflect differences in the genetic background of the two strains [62]. We previously demonstrated that the size of the alum-induced granuloma in rats is dramatically influenced by their genetic background, the granuloma being much smaller in Lewis rats with Th1 biased immune responses compared to Sprague–Dawley rats with balanced Th1/Th2 immunity [45]. The C57BL/6 mouse strain is known to exhibit a Th1-prone, pro-inflammatory type response to injury [63,64]. To our knowledge, the T helper immunity status of CD1 mice is not known. Interestingly, C57BL/6 mice produce more MCP-1/CCL2 than other strains [64], and this major inflammatory monocyte chemoattractant is crucially involved in both systemic biodistribution and neurodelivery of Al particles captured by monocyte-lineage cells [39]. Notably, increased circulating MCP-1/CCL2 is the sole identified biomarker in myalgic encephalomyelitis patients with MMF [65]. Moreover, human MMF is mainly observed in middle aged or elderly individuals, a time when MCP-1/CCL2 production increases and immuno-senescence occurs [66]. Clarification of the influence of mouse strains Th1 and Th2-biased immune responses in AluDia brain translocation clearly deserves future studies.

In previous published studies, motor and behavioural impairments were observed following sc (behind the neck) Alhydrogel<sup>®</sup> injection to CD1 mice with doses of 100 and 300 µg Al/kg [17,41]. These effects were associated with Al deposits in the central nervous system (spinal cord) assessed by Morin stain. To examine if the route of exposure may represent an important factor for alum toxicity, a nested study was conducted herein, showing that alum particles may penetrate the brain at D45 after the sc (and not im) injection, performed at the dose of 200 µg Al/kg (and not at the dose of 400 µg Al/kg). A higher rate of brain translocation after sc injection may be explained by a much higher density of dendritic cells with high migrating properties, in the skin compared to muscle. The fact that half dose

resulted in brain translocation, which was not observed at higher dose, is reminiscent of the non monotonic dose/response curves previously observed with environmental toxins, including particulate compounds [67]. In another study, we similarly observed neurobehavioural changes at 200 but not 400  $\mu\text{g Al/kg}$  (Crépeaux *et al.*, manuscript in preparation). The exact significance of such observations is unknown, but one may speculate that huge quantities of alum injected in the tissue may induce blockade of critical macrophage functions such as migration and xeno/autophagic disposition of particles, as previously reported for infectious particles [37].

## 5. Conclusion

We observed a strikingly delayed, previously unknown, systemic translocation of alum particles injected into muscle, with conspicuous alum accumulations in the lymphatic system and spleen 9 months after injection. In addition to the crucial ‘t’ factor, our results strongly suggest the influence of the mouse strain, the dose and the route of administration on alum biodisposition. All these parameters should be taken into account in the design of future alum toxicological studies.

### List of abbreviations

AluDia: aluminium-nanodiamonds complex

ASIA: autoimmune/auto-inflammatory syndrome induced by adjuvants

dLNs: draining lymph nodes

FDA: food and drug administration

HBV: hepatitis B virus

HPG: hyperbranched polyglycerol

HPHT: High Pressure High Temperature

im: intramuscular

fNDs: fluorescent nanodiamonds

MMF: macrophagic myofasciitis

MCP-1/CCL2: monocyte chemoattractant protein 1/Chemokine Ligand 2

PBS: phosphate buffer saline

TA: *tibialis anterior*

THGA: spectrometer with a transversely heated graphite atomizer

TH GFAAS: graphite furnace atomic absorption

Th1 & Th2: T helper 1 & 2

sc: subcutaneous

### **Conflicts of interest**

The authors declare that there are no conflicts of interest.

### **Acknowledgements**

The authors thank Marina Bermudez de Castro Rubio, Anthony Deust and Frédéric Ros for their technical help, and Marie De Antonio for her statistical explanations. This study was supported by the University of British Columbia in Vancouver, the Dvoskin Family Foundation, ANSM, and Région Ile-de-France DIM NeRF (“Nano-in-brain” project).

## References

- [1] C. Exley, Human exposure to aluminium, *Environ. Sci. Process. Impacts*. 15 (2013) 1807–1816.
- [2] C. Exley, L. Swarbrick, R.K. Gherardi, F.-J. Authier, A role for the body burden of aluminium in vaccine-associated macrophagic myofasciitis and chronic fatigue syndrome, *Med. Hypotheses*. 72 (2009) 135–139.
- [3] M. Kawahara, Effects of aluminum on the nervous system and its possible link with neurodegenerative diseases, *J. Alzheimer Dis.* 8 (2005) 171-182.
- [4] S. Bondy, The neurotoxicity of environmental aluminum is still an issue, *Neurotoxicology* 31 (2010) 575–581.
- [5] S. Kumar, Biphasic effect of aluminium on cholinergic enzyme of rat brain, *Neurosci. Lett.* 248 (1998) 121–123.
- [6] L. Tomljenovic, C.A. Shaw, Do aluminum vaccine adjuvants contribute to the rising prevalence of autism?, *J. Inorg. Biochem.* 105 (2011) 1489–1499.
- [7] C. Exley, What is the risk of aluminium as a neurotoxin?, *Expert Rev. Neurother.* 14 (2014) 589–591.
- [8] P. Zatta, M. Ibn-Lkhatat-Idrissi, P. Zambenedetti, M. Kilyen, T. Kiss, In vivo and in vitro effects of aluminum on the activity of mouse brain acetylcholinesterase, *Brain Res. Bull.* 59 (2002) 41–45.
- [9] S.V. Verstraeten, L. Aimo, P.I. Oteiza, Aluminium and lead: molecular mechanisms of brain toxicity, *Arch. Toxicol.* 82 (2008) 789–802.
- [10] R. Moumen, N. Ait-Oukhatar, F. Bureau, C. Fleury, D. Bouglé, P. Arhan, *et al.*, Aluminium increases xanthine oxidase activity and disturbs antioxidant status in the rat, *J. Trace Elem. Med. Biol. Organ Soc. Miner. Trace Elem. GMS.* 15 (2001) 89–93.
- [11] P. Nayak, Aluminum: impacts and disease, *Environ. Res.* 89 (2002) 101–115.

- [12] R.A. Yokel, Brain uptake, retention, and efflux of aluminum and manganese, *Environ. Health Perspect.* 110 Suppl 5 (2002) 699–704.
- [13] C. Exley, When an aluminium adjuvant is not an aluminium adjuvant used in human vaccination programmes, *Vaccine.* 30 (2012) 2042.
- [14] S. Sánchez-Iglesias, R. Soto-Otero, J. Iglesias-González, M.C. Barciela-Alonso, P. Bermejo-Barrera, E. Méndez-Alvarez, Analysis of brain regional distribution of aluminium in rats via oral and intraperitoneal administration, *J. Trace Elem. Med. Biol. Organ Soc. Miner. Trace Elem. GMS.* 21 Suppl 1 (2007) 31–34.
- [15] H. Rosenblum, Y. Shoenfeld, H. Amital, The common immunogenic etiology of chronic fatigue syndrome: from infections to vaccines via adjuvants to the ASIA syndrome, *Infect. Dis. Clin. North Am.* 25 (2011) 851–863.
- [16] M.A. Hernán, S.S. Jick, M.J. Olek, H. Jick, Recombinant hepatitis B vaccine and the risk of multiple sclerosis: a prospective study, *Neurology.* 63 (2004) 838–842.
- [17] M.S. Petrik, M.C. Wong, R.C. Tabata, R.F. Garry, C.A. Shaw, Aluminum adjuvant linked to Gulf War illness induces motor neuron death in mice, *Neuromolecular Med.* 9 (2007) 83–100.
- [18] Y. Shoenfeld, N. Agmon-Levin, "ASIA"- autoimmune/inflammatory syndrome induced by adjuvants, *J Autoimmunity* 36 (1) (2011) 4-8.
- [19] S.J. van Rensburg, F.C. Potocnik, T. Kiss, F. Hugo, P. van Zijl, E. Mansvelt, *et al.*, Serum concentrations of some metals and steroids in patients with chronic fatigue syndrome with reference to neurological and cognitive abnormalities, *Brain Res. Bull.* 55 (2001) 319–325.
- [20] A. Lerner, Aluminum as an adjuvant in Crohn's disease induction, *Lupus.* 21 (2012) 231–238.

- [21] P. De Sole, C. Rossi, M. Chiarpotto, G. Ciasca, B. Bocca, A. Alimonti, *et al.*, Possible relationship between Al/ferritin complex and Alzheimer's disease, *Clin. Biochem.* 46 (2013) 89–93.
- [22] R. K. Gherardi, M. Coquet, P. Chérin *et al.*, “Macrophagic myofasciitis: an emerging entity,” *The Lancet* 352 (1998) 347–352.
- [23] World Health Organization Vaccine Safety Advisory Committee, Macrophagic myofasciitis and aluminum-containing vaccines, *Wkly Epidemiol. Rec.* 74 (1999) 338–340.
- [24] M. Couette, M.-F. Boisse, P. Maison, P. Brugieres, P. Cesaro, X. Chevalier, *et al.*, Long-term persistence of vaccine-derived aluminum hydroxide is associated with chronic cognitive dysfunction, *J. Inorg. Biochem.* 103 (2009) 1571–1578.
- [25] E. Passeri, C. Villa, M. Couette, E. Itti, P. Brugieres, P. Cesaro, *et al.*, Long-term follow-up of cognitive dysfunction in patients with aluminum hydroxide-induced macrophagic myofasciitis (MMF), *J. Inorg. Biochem.* 105 (2011) 1457–1463.
- [26] R.K. Gherardi, F.J. Authier, Macrophagic myofasciitis: characterization and pathophysiology, *Lupus.* 21 (2012) 184–189.
- [27] T. Santiago, O. Rebelo, L. Negrão, A. Matos, Macrophagic myofasciitis and vaccination: Consequence or coincidence?, *Rheumatol. Int.* 35 (2014) 189-192.
- [28] F.J. Authier, P. Cherin, A. Creange, B. Bonnotte, X. Ferrer, A. Abdelmoumni, *et al.*, Central nervous system disease in patients with macrophagic myofasciitis, *Brain J. Neurol.* 124 (2001) 974–983.
- [29] R.K. Gherardi, M. Coquet, P. Cherin, L. Belec, P. Moretto, P.A. Dreyfus, *et al.*, Macrophagic myofasciitis lesions assess long-term persistence of vaccine-derived aluminium hydroxide in muscle, *Brain J. Neurol.* 124 (2001) 1821–1831.
- [30] N. Rangunathan-Thangarajah, C. Le Beller, P. Boutouyrie, G. Bassez, R.K. Gherardi, S. Laurent, *et al.*, Distinctive clinical features in arthro-myalgic patients with and without

aluminum hydroxyde-induced macrophagic myofasciitis: an exploratory study, *J. Inorg. Biochem.* 128 (2013) 262–266.

[31] C. Exley, P. Siesjö, H. Eriksson, The immunobiology of aluminium adjuvants: how do they really work?, *Trends Immunol.* 31 (2010) 103–109.

[32] C.A. Shaw, L. Tomljenovic, Aluminum in the central nervous system (CNS): toxicity in humans and animals, vaccine adjuvants, and autoimmunity, *Immunol. Res.* 56 (2013) 304–316.

[33] A.T. Glenny, C.G. Pope, H. Waddington, U. Wallace, XXIII-the antigenic value of toxoid precipitated by potassium alum, *J. Pathol Bacteriol.* 29 (1926) 38-39.

[34] T.C. Eickhoff, M. Myers, Conference report: Workshop summary Aluminum in vaccines, *Vaccine* 20 (2002) S1–S4.

[35] Y. Kashiwagi, M. Maeda, H. Kawashima, T. Nakayama, Inflammatory responses following intramuscular and subcutaneous immunization with aluminum-adjuvanted or non-adjuvanted vaccines, *Vaccine.* 32 (2014) 3393–3401.

[36] S. Hutchinson, R.A. Benson, V.B. Gibson, A.H. Pollock, P. Garside, J.M. Brewer, Antigen depot is not required for alum adjuvanticy, *Faseb J* (2012) 26: 1272-1279.

[37] R.K. Gherardi, H. Eidi, G. Crépeaux, F.J. Authier, J. Cadusseau, Biopersistence and brain translocation of aluminum adjuvants of vaccines, *Front. Neurol.* 6 (2015) 4.

[38] R. Flarend, T. Bin, D. Elmore, S.L. Hem, A preliminary study of the dermal absorption of aluminium from antiperspirants using aluminium-26, *Food Chem. Toxicol. Int. J. Publ. Br. Ind. Biol. Res. Assoc.* 39 (2001) 163–168.

[39] Z. Khan, C. Combadière, F.-J. Authier, V. Itier, F. Lux, C. Exley, *et al.*, Slow CCL2-dependent translocation of biopersistent particles from muscle to brain, *BMC Med.* 11 (2013) 99.

- [40] H. Eidi, M.O. David, G. Crépeaux, L. Henry, V. Joshi, M.H. Berger, M. Sennour, J. Cadusseau, R.K. Gherardi, P.A. Curmi, Fluorescent nanodiamonds as a relevant tag for the assessment of alum adjuvant particle biodisposition, *BMC Medicine* in press.
- [41] C.A. Shaw, M.S. Petrik, Aluminum hydroxide injections lead to motor deficits and motor neuron degeneration, *J. Inorg. Biochem.* 103 (2009) 1555–1562.
- [42] L. Luján, M. Pérez, E. Salazar, N. Álvarez, M. Gimeno, P. Pinczowski, *et al.*, Autoimmune/autoinflammatory syndrome induced by adjuvants (ASIA syndrome) in commercial sheep, *Immunol. Res.* 56 (2013) 317–324.
- [43] N. Agmon-Levin, M.-T. Arango, S. Kivity, A. Katzav, B. Gilburd, M. Blank, *et al.*, Immunization with hepatitis B vaccine accelerates SLE-like disease in a murine model, *J. Autoimmun.* 54 (2014) 21–32.
- [44] F. Verdier, R. Burnett, C. Michelet-Habchi, P. Moretto, F. Fievet-Groyne, E. Sauzeat, Aluminium assay and evaluation of the local reaction at several time points after intramuscular administration of aluminium containing vaccines in the *Cynomolgus* monkey, *Vaccine* 23 (2005) 1359–1367.
- [45] F.-J. Authier, S. Sauvat, C. Christov, P. Chariot, G. Raisbeck, M.-F. Poron, *et al.*, ALOH<sub>3</sub>-adjuvanted vaccine-induced macrophagic myofasciitis in rats is influenced by the genetic background, *Neuromuscul. Disord. NMD.* 16 (2006) 347–352.
- [46] European Union Directive, European Union Directive, 2010/63/EU of 22 September 2010 on the Approximation of Laws, Regulations and Administrative Provisions of the Member States Regarding the Protection of Animals Used for Experimental and Other Scientific Purposes.
- [47] J.P. Boudou, P.A. Curmi, F. Jelezko, J. Wrachtrup, P. Aubert, M. Sennour, G. Balasubramanian, R. Reuter, A. Thorel, E. Gaffet, High yield fabrication of fluorescent nanodiamonds, *Nanotechnology* 20 (2009) 235602.

- [48] J.P. Boudou, M.O. David, V. Joshi, H. Eidi, P.A. Curmi, Hyperbranched Polymers : Structure of Hyperbranched Polyglycerol and Amphiphilic Poly(glycerol ester)s in Dilute Aqueous and Nonaqueous Solution, *Diamond RelatMat* 37 (2013) 131-138.
- [49] E. House, M. Esiri, G. Forster, P.G. Ince, C. Exley, Aluminium, iron and copper in human brain tissues donated to the Medical Research Council's Cognitive Function and Ageing Study, *Met. Integr. Biometal Sci.* 4 (2012) 56–65.
- [50] R.N. Walsh, R.A. Cummins, The Open-Field Test: a critical review, *Psychol. Bull.* 83 (1976) 482–504.
- [51] J.K. Shepherd, S.S. Grewal, A. Fletcher, D.J. Bill, C.T. Dourish, Behavioural and pharmacological characterisation of the elevated “zero-maze” as an animal model of anxiety, *Psychopharmacology (Berl.)*. 116 (1994) 56–64.
- [52] L. Coutellier, A.-C. Friedrich, K. Failing, V. Marashi, H. Würbel, Effects of foraging demand on maternal behaviour and adult offspring anxiety and stress response in C57BL/6 mice, *Behav. Brain Res.* 196 (2009) 192–199.
- [53] A. Ennaceur, J. Delacour, A new one-trial test for neurobiological studies of memory in rats. 1: Behavioral data, *Behav. Brain Res.* 31 (1988) 47–59.
- [54] P.A. Dudchenko, An overview of the tasks used to test working memory in rodents, *Neurosci. Biobehav. Rev.* 28 (2004) 699–709.
- [55] A. Ennaceur, One-trial object recognition in rats and mice: methodological and theoretical issues, *Behav. Brain Res.* 215 (2010) 244–254.
- [56] S.J. Moore, K. Deshpande, G.S. Stinnett, A.F. Seasholtz, G.G. Murphy, Conversion of short-term to long-term memory in the novel object recognition paradigm, *Neurobiol. Learn. Mem.* 105 (2013) 174–185.
- [57] W. Kondziela, Eine neue method zur messung der muskularen relaxation bei weissen mausen. *Arch. Int. Pharmacodyn.* 152 (1964) 277-84.

- [58] J.P.J. Maurissen, B.R. Marable, A.K. Andrus, K.E. Stebbins, Factors affecting grip strength testing, *Neurotoxicol. Teratol.* 25 (2003) 543–553.
- [59] M. Pratte, N. Panayotis, A. Ghata, L. Villard, J.-C. Roux, Progressive motor and respiratory metabolism deficits in post-weaning *Mecp2*-null male mice, *Behav. Brain Res.* 216 (2011) 313–320.
- [60] L. Steru, R. Chermat, B. Thierry, P. Simon, The tail suspension test: a new method for screening antidepressants in mice, *Psychopharmacology (Berl.)*. 85 (1985) 367–370.
- [61] E.F. Espejo, D. Mir, Structure of the rat's behaviour in the hot plate test, *Behav. Brain Res.* 56 (1993) 171–176.
- [62] C.D. Mills, K. Kincaid, J.M. Alt, M.J. Heilman, A.M. Hill, M-1/M-2 macrophages and the Th1/Th2 paradigm, *J. Immunol.* 164 (2000) 6166–6173.
- [63] G.S. Whitehead, J.K.L. Walker, K.G. Berman, W.M. Foster, D.A. Schwartz, Allergen-induced airway disease is mouse strain dependent, *Am. J. Physiol. Lung Cell. Mol. Physiol.* 285 (2003) L32–L42.
- [64] C.D. Mills, K. Ley, M1 and M2 macrophages: the chicken and the egg of immunity, *J. Innate Immun.* 6 (2014) 716–726.
- [65] J. Cadusseau, N. Rangunathan-Thangarajah, M. Surenaud, S. Hue, F.-J. Authier, R.K. Gherardi, Selective elevation of circulating CCL2/MCP1 levels in patients with longstanding post-vaccinal macrophagic myofasciitis and ASIA, *Curr. Med. Chem.* 21 (2014) 511–517.
- [66] A.S. Mansfield, W.K. Nevala, R.S. Dronca, A.A. Leontovich, L. Shuster, S.N. Markovic, Normal ageing is associated with an increase in Th2 cells, MCP-1 (CCL2) and RANTES (CCL5), with differences in sCD40L and PDGF-AA between sexes, *Clin. Exp. Immunol.* 170 (2) (2012) 186–93.
- [67] I. Iavicoli, L. Fontana, V. Leso, E.J. Calabrese, Hormetic dose-responses in nanotechnology studies, *Sci. Total Environ.* 487 (2014) 361–374.

**Fig. 1.** AluDia accumulation in inguinal dLNs (a,b, f,g) and spleen (c,d,h,i) following AluDia im injection in *tibialis anterior* muscle (400  $\mu$ g Al/kg) at D45 (a-e) and at D270 (f-j).

a, c, f, h: The red specific fluorescence of AluDia excited by a 532 nm laser source.

b, d, g, i: phase contrast.

e and j: AluDia luminescence spectrum with a specific peak at 700 nm.

**Fig. 2.** AluDia in brain (animal 1: a, b, c; animal 2: d, e, f) following AluDia sc injection (200  $\mu\text{g Al/kg}$ ) at D45.

a and d: The red specific fluorescence of AluDia excited by a 532 nm laser source.

b and e: phase contrast.

c and f: AluDia luminescence spectrum with a specific peak at 700 nm

Table 1

A semi-quantitative study of the progressive decrease of granuloma size in injected muscle with Alhydrogel or HBV vaccine.

Group	Days	No granuloma (0)	Small granuloma (+)	Medium granuloma (++)	Large granuloma (+++)	Total granuloma
Alhydrogel® 400 µg Al/kg, im	D45	7%	14%	46%	32%	93%
	D135	35%	21%	18%	26%	65%
	D180	24%	28%	43%	5%	76%
	D270	65%	18%	10%	6%	35%
HBV vaccine® 400 µg Al/kg, im	D45	32%	42%	22%	4%	67%
	D135	21%	35%	31%	13%	79%
	D180	35%	41%	25%	0%	65%
	D270	69%	25%	6%	0%	31%

According to their size, observed granulomas were divided to four types: without granuloma (0), small (+), medium (++) and large (+++) granuloma. Then, percentage of each size in observed muscles was calculated, for n = 3 animals per group.

Table 2

A qualitative study of the translocation of AluDia particles following intramuscular injections at the dose of 400  $\mu\text{g}$  Al/kg, 45, 135, 180 or 270 days after injections.

AluDia	Particle counts						
	Ing DLNs			Spleen			Brain mean
	mean	$\pm$	sd	mean	$\pm$	sd	
D45	1145	$\pm$	87	15	$\pm$	3	0
D135	3820	$\pm$	123	55	$\pm$	12	0
D180	7372	$\pm$	194	177	$\pm$	32	0
D270	115478	$\pm$	377	785	$\pm$	61	0

Results are expressed as mean  $\pm$  S.D. of n = 3 mice/group per organ and per time point.

Ing dLNs, Inguinal draining lymph nodes.

Table 3

Aluminum cerebral concentration measured by furnace atomic absorption spectrometry ( $\mu\text{g/g}$  of dry weight).

Cerebral Al concentration	Control	Alhydrogel® group 400 $\mu\text{g}$ Al/kg, im	HBV vaccine group 400 $\mu\text{g}$ Al/kg, im	Kruskal-Wallis test
D45	0.54095 (0.3250 - 1.4837)	0.57335 (0.0234 - 8.8778)	0.90625 (0.6104 - 1.3623)	n.s.
D135	0.02485 (0.0179 - 0.1877)	0.4317 (0.0200 - 33.3432)	0.6843 (0.1214 - 1.2061)	n.s.
D180	0.0956 (0.0174 - 0.8776)	0.0143 (0.0133 - 0.3540)	0.0451 (0.0158 - 0.6317)	n.s.
D270	1.0534 (0.3975 - 2.8053)	0.01495 * (0.0123 - 0.1859)	0.0141 * (0.0122 - 0.0206)	p < 0.05

Results are expressed as median and quartiles (in brackets) of  $n = 5$  brains/group. Non parametric Kruskal-Wallis test followed by a Mann-Whitney procedure was used for multiple comparisons.

\*  $p < 0.05$ , statistical significant difference from controls.

Table 4

A qualitative study of the translocation of AluDia particles following intramuscular or subcutaneous injections at the doses of 200 or 400  $\mu\text{g}/\text{kg}$ , 45 days after injections.

AluDia	Particle counts			
	im 200 $\mu\text{g Al}/\text{kg}$	im 400 $\mu\text{g Al}/\text{kg}$	sc 200 $\mu\text{g Al}/\text{kg}$	sc 400 $\mu\text{g Al}/\text{kg}$
Brain	0	0	15 $\pm$ 7	0

Results are expressed as mean  $\pm$  S.D. of  $n = 4$  mice/group per organ and per time point.

Im, intramuscular; sc, subcutaneous.

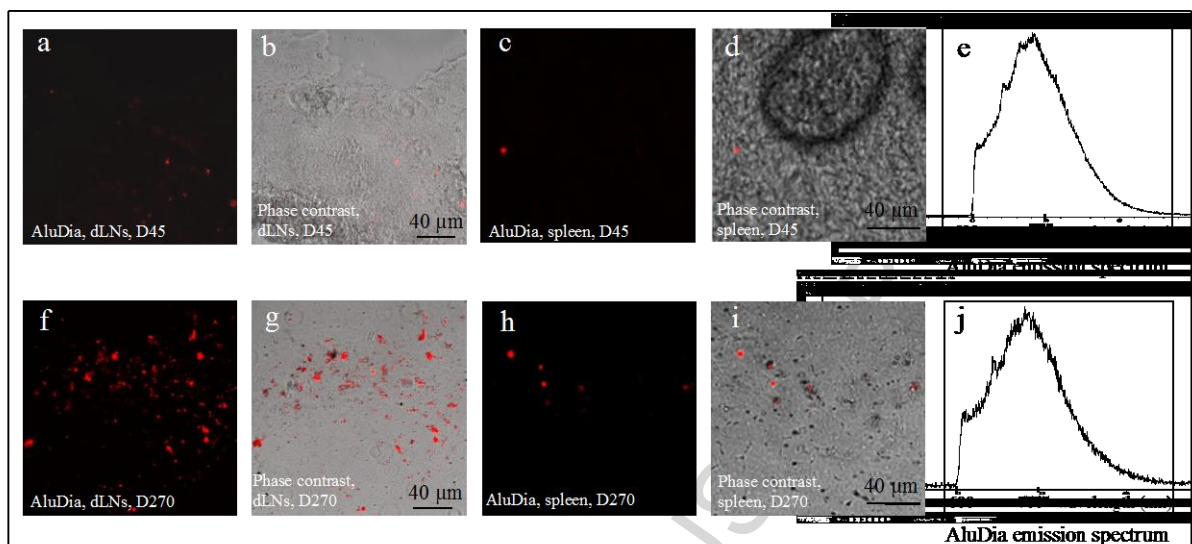


**Fig. 1.** AluDia accumulation in inguinal dLNs (a,b, f,g) and spleen (c,d,h,i) following AluDia im injection in *tibialis anterior* muscle (400 μg Al/kg) at D45 (a-e) and at D270 (f-j).

a, c, f, h: The red specific fluorescence of AluDia excited by a 532 nm laser source.

b, d, g, i: phase contrast

e and j: AluDia luminescence spectrum with a specific peak at 700 nm.

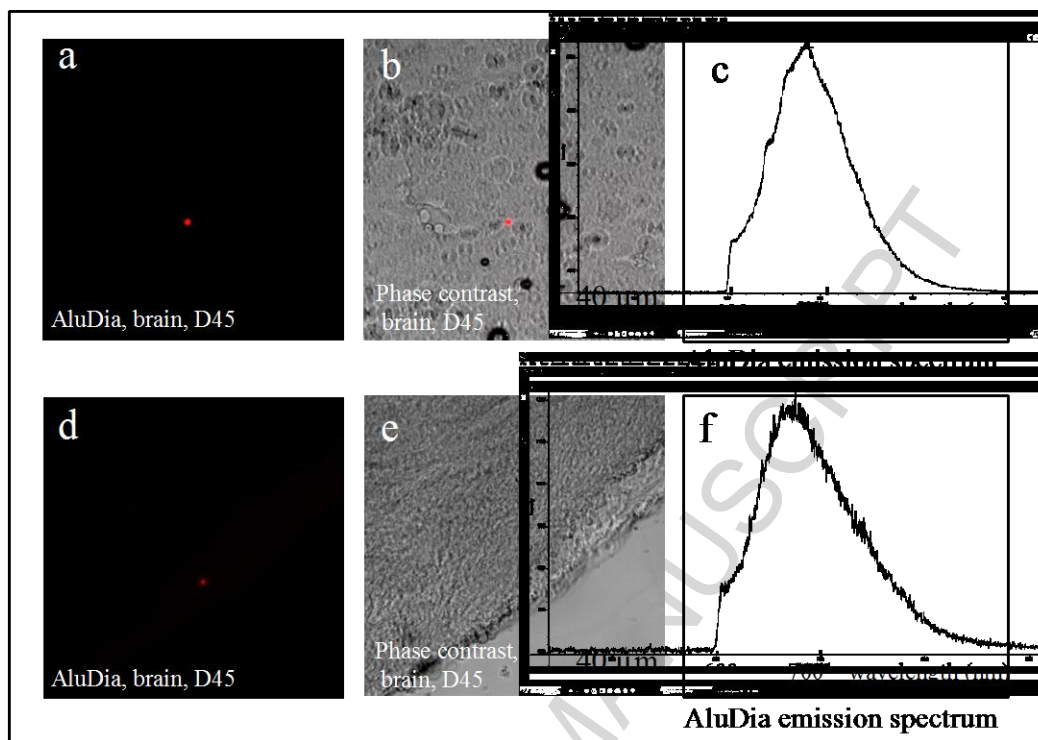
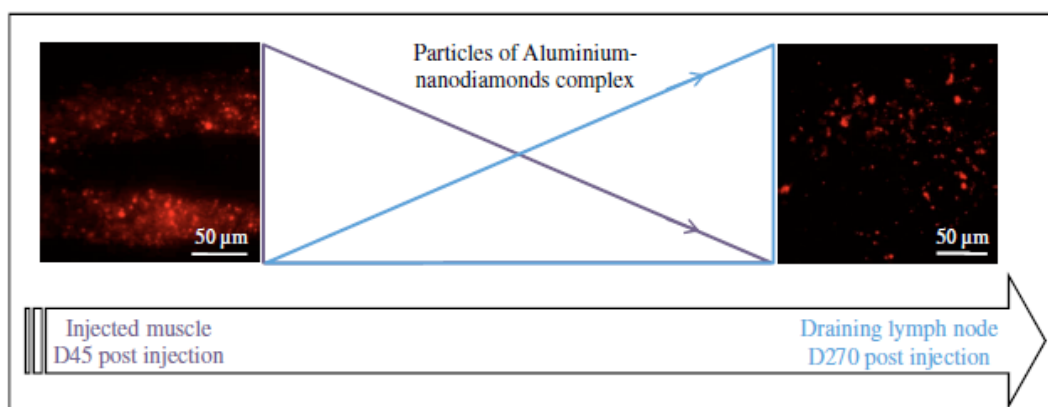


**Fig. 2.** AluDia in brain (animal 1: a, b, c; animal 2: d, e, f) following AluDia sc injection ( $200 \mu\text{g Al/kg}$ ) at D45.

a and d: The red specific fluorescence of AluDia excited by a 532 nm laser source.

b and e: phase contrast.

c and f: AluDia luminescence spectrum with a specific peak at 700 nm



Graphical Abstract

ACCEPTED MAN

### Highlights

- Vaccine safety is a key question due to reported adverse events in humans & animals
- Results showed a highly delayed systemic translocation of adjuvant particles
- This study suggests the importance of mouse strain, route of exposure & doses
- This study confirms the striking biopersistence of alum